J. Electroanal. Chem., 171 (1984) 139–155
Elsevier Sequoia S.A., Lausanne – Printed in The Netherlands

THE CATALYSIS OF THE REDUCTION OF Zn(II) IONS BY IODIDE IONS

A MECHANISTIC STUDY IN MIXED 1 *M* $NaClO_4$/NaI AQUEOUS SOLUTIONS

R. ANDREU

Department of Physical Chemistry, The University, Palos de la Frontera 1, Sevilla (Spain)

M. SLUYTERS-REHBACH and J.H. SLUYTERS

Van 't Hoff Laboratory of Physical and Colloid Chemistry, State University, Padualaan 8, 3584 CH Utrecht (The Netherlands)

(Received 15th December 1983)

ABSTRACT

The two-step reduction of Zn(II) ions at the dropping mercury electrode in 1 *M* $NaClO_4$/NaI mixtures is studied by the impedance method. Both steps are found to be catalysed, the increase in the logarithm of the rate constant being proportional to the surface excess of I^-.

Attempts are made to interpret the results quantitatively with existing models and the applicability of these models to this electrode reaction is discussed.

INTRODUCTION

In spite of the fact that the Zn^{2+} reduction on mercury constitutes one of the most extensively studied reactions in electrochemistry, it is only rather recently that attention has also been paid to the multi-step nature of its mechanism [1–4].

Some earlier work was devoted to the analysis of the accelerating effect that iodide ions exert on this reaction [5–11] and, although some disagreement about the adequacy of its interpretation arose, a linear correlation between activation energy and amount of specifically adsorbed iodide was well established.

To provide a theoretical link relating kinetic and adsorption parameters, a number of models, beyond the classical Frumkin effect, were developed [12–17], and in some cases a satisfactory account of iodide catalysis was given, although a one-step two-electron transfer was assumed.

Later, Eriksrud [18] described the multi-step reduction of Zn^{2+} in mixtures of KI + KCl at a constant ionic strength. She found a higher enhancement of the rate of the second electron transfer than of that of the first electron transfer, on exchanging chloride by iodide. As chloride is known to interact strongly with Zn^{2+}

0022-0728/84/$03.00

cations, its presence thus introducing an additional (and sometimes undesirable) difficulty in the analysis of the results, it seemed worthwhile to consider the effect of iodide on the deposition of Zn^{2+} in the presence of a non-complexing electrolyte.

In this report, the kinetics of Zn^{2+} reduction in $NaClO_4 + NaI$ mixtures are examined by the impedance technique. The rate constants of the two separate electron-transfer steps are derived, and their dependence on the amount of specifically adsorbed iodide is expressed by a simple mathematical relationship. These results are compared with the predictions derived from the above-mentioned models.

EXPERIMENTAL

Measurements were performed in a three-electrode cell, with a mercury pool as counter electrode, a DME and a sodium-chloride-saturated calomel electrode (SSCE).

Solutions were made up from double-distilled water and analytical-grade reagents. The zinc perchlorate was prepared by dissolving ZnO in a small excess of perchloric acid to make the final solution 10^{-3} M in H^+. In order to achieve the desired accuracy over a ~ 350 mV potential range the cell impedance was measured at two concentrations of Zn^{2+} viz. 4 and 20 mM.

Oxygen was removed from the solution by bubbling argon, which had been purified by passage through a B.T.S. catalyst. The cell and reference electrode were kept at $25 \pm 0.1°C$. Cell impedance and dc polarograms were measured with the network analyser system described previously [19], at 4 s after drop birth. If necessary, the dc potential was corrected to take account of the ohmic drop in the cell.

KINETIC ANALYSIS

In-phase and quadrature components of the cell impedance were measured at 16 frequencies in the range 80–10.000 Hz. The ohmic resistance of the solution was determined at 10 kHz outside the faradaic region.

Frequency analysis of the interfacial admittance proved to be consistent with the Randles equivalent circuit and provided values of the charge transfer resistance R_{ct} and the Warburg coefficient σ, from which the cathodic rate constant k_f was derived [20] as a function of dc potential E.

Using Koutecký's equation for diffusion-limiting currents, the dc polarograms gave a value of 6.8×10^{-6} cm^2 s^{-1} for the diffusion coefficient D_O of Zn^{2+}. The analogous value for Zn in mercury (D_R) was selected from the literature: 1.6×10^{-5} cm^2 s^{-1} [21].

A first estimate of the reversible half-wave potential was obtained by extrapolation of the reversible part of the wave to $\ln[I/(I_d - I)] = 0$, in the $\ln[I/(I_d - I)]$ vs. E plot. An optimal value of -0.990 V (SSCE) was selected from the dc potential dependence of R_{ct} and σ.

It is interesting to point out that both D_O and $E^r_{1/2}$ were found to be independent of the solution composition for the mixtures considered.

DOUBLE LAYER ANALYSIS

Sodium perchlorate was considered as a non-specifically adsorbed electrolyte at the potentials where the Zn^{2+} reduction takes place ($E < -0.90$ V). The amount of specifically adsorbed iodide (q^i) was interpolated from Grahame's data for pure KI [22], making use of the previous finding [23] that, at a given salt activity and charge density on the metal (q^M), q^i is identical for the one molar ionic-strength mixtures and the pure salt solutions.

It was further assumed that replacement of K^+ by Na^+ does not change the adsorbability of iodide.

The required q^M values were obtained by back-integration from -1.550 V ($q^M = -20.6$ μC cm^{-2}) of the capacity vs. potential curves, measured at 1020 Hz.

The potential at the outer Helmholtz plane (OHP), ϕ_2, and at a plane 0.28 nm further into the diffuse layer, ϕ_{1H_2O}, were calculated according to classical Gouy–Chapman theory [24].

RESULTS AND DISCUSSION

Mathematical description of the iodide catalysis

Frequency analysis of the cell impedance allowed derivation of the cathodic rate constant values for the Zn^{2+} reduction in the potential range -0.90 V to -1.26 V (SSCE). Similar results to those previously published [20] were obtained in the absence of iodide (see Table 1).

The accelerating influence of iodide on the reaction rate is illustrated in Fig. 1. At the most negative potentials, where specific adsorption of iodide is absent, the $\ln k_f$ vs. E plots for the iodide + perchlorate mixtures become identical to that obtained for pure perchlorate.

The catalytic influence of iodide can be better described on a $\ln k_f$ (at a given E) vs. $-q^i$ plot, such as Fig. 2. At a given potential, $\ln k_f$ increases linearly with the amount of specifically adsorbed iodide. The slope of such plots appears to be potential independent for $E \leqslant -1.02$ V and equal to 0.63 (± 0.03) μC^{-1} cm^2. At more positive potentials, a continuous decrease of the slope is observed down to 0.38 μC^{-1} cm^2 at $E = -0.90$ V.

Such an increase in the reduction rate with iodide concentration cannot be accounted for by a classical Frumkin correction in which the reaction plane is located at the OHP, as becomes evident after inspection of Fig. 3. Moreover, the Frumkin corrected rate constants ($k_f^l = k_f \exp(2f\phi_2)$) show a strong dependence on the solution composition, and the plots of $\ln k_f^l$ (at given $E - \phi_2$) vs. $-q^i$ still display a linear behaviour with slopes ranging from 0.46 to 0.34 μC^{-1} cm^2 (Fig. 4).

In view of the low coverages with iodide encountered at the potentials of interest ($-q^i < 7.5$ μC cm^{-2} whereas $-q^i_{max} = 87$ μC cm^{-2}), it is unlikely that the smaller slopes in the $\ln k_f$ vs $-q^i$ plots, observed in Figs. 2 and 4 at the more positive potentials, should be explained by some blocking effect [12]. A more reasonable

explanation can be based on the idea that the charge transfer proceeds via two consecutive one-electron transfer steps, as has been clearly demonstrated to apply in the case of the pure perchlorate supporting electrolyte [20]. The conclusion is then that the accelerating influence of the iodide ions is stronger on the first step than on the second, since the former dominates at more negative potentials.

At the most negative potentials, where the first electron transfer is rate determining, we have $k_f = k_1$, and the iodide catalysis at a given potential satisfies the expression:

$$\ln k_1 = \ln k_{10} - Aq^i \tag{1}$$

where A is independent of the potential and the iodide concentration, and k_{10} represents the rate constant of the first electron transfer in the presence of 1 M $NaClO_4$ at the same potential.

At more positive potentials the overall rate is determined by both steps simulta-

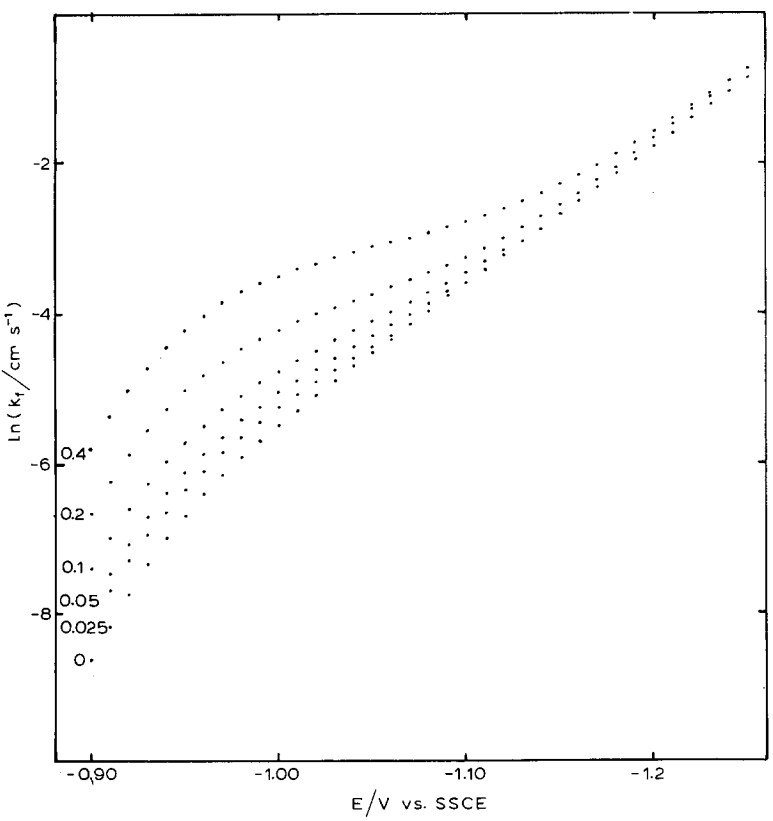

Fig. 1. The potential dependence of the overall forward reaction rate constant of the Zn(II) reduction in $(1-x)$ M $NaClO_4$ + x M KI mixed electrolyte solutions for some indicated values of x.

neously. If eqn. (1) is assumed to remain valid at these potentials, we can use it to calculate the rate constant k_2 of the second step, which appears to satisfy a similar expression:

$$\ln k_2 = -\ln[1/k_f - 1/k_1] = \ln k_{20} - Bq^i \tag{2}$$

It thus becomes possible to describe the catalytic influence of iodide on the Zn^{2+} reduction by means of A and B, according to:

$$\frac{1}{k_f} = \frac{\exp(Aq^i)}{k_{10}} + \frac{\exp(Bq^i)}{k_{20}} = \frac{\exp(Aq^i)}{k_{s1}\exp(-\alpha_1^a f(E - E_f^\circ))} + \frac{\exp(Bq^i)}{k_{s2}\exp(-(1+\alpha_2^a)f(E - E_f^\circ))} \tag{3}$$

where α_1^a and α_2^a are the individual transfer coefficients and $f = F/RT$. Table 1 reproduces the whole set of parameters which fit the data of Fig. 1 to eqn. (3) and the values that apply to Frumkin-corrected rate constants, both when the reaction plane is located at the OHP and at 0.28 nm further into the diffuse layer.

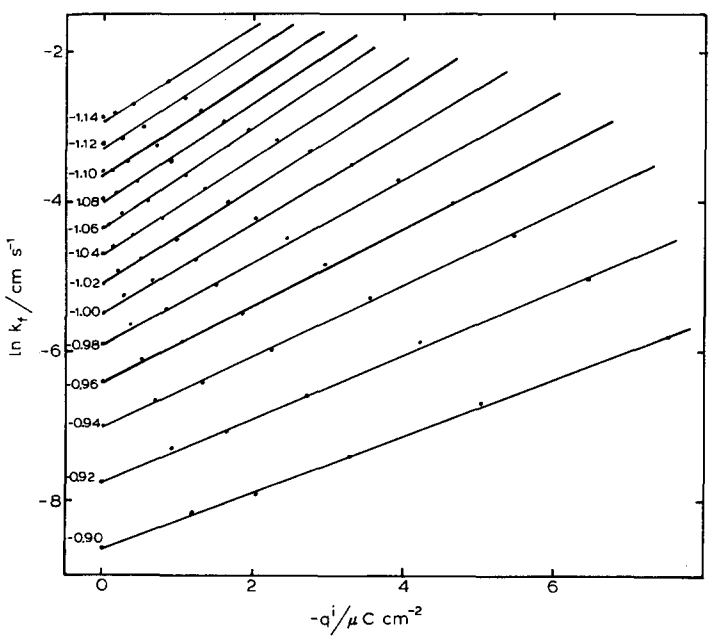

Fig. 2. The relationship between the forward reaction rate constant and the amount of specifically adsorbed anion at some indicated electrode potentials in V vs. SSCE.

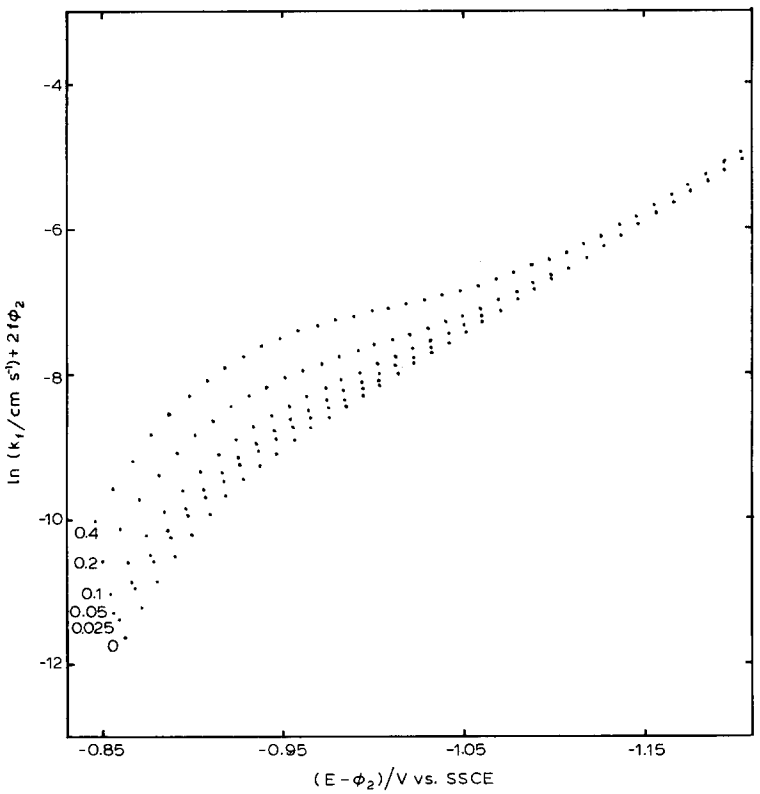

Fig. 3. As Fig. 1, after application of the diffuse double layer correction.

TABLE 1

Parameters fitting the data of Fig. 1 and values applying to Frumkin-corrected rate constant at 0.28 nm from and at OHP

Non-corrected data	Frumkin-corrected	
	At 0.28 nm from OHP	At OHP
E_f° [a] $= -0.995$ V	$E_f^{\circ} - \phi^{\circ}_{1H_2O} = -0.978$ V	$E_f^{\circ} - \phi_2^{\circ} = -0.951$ V
$k_{s1} = 0.0040$ cm s^{-1}	$(k^t_{s1})_{1H_2O} = 0.0011$ cm s^{-1}	$k^t_{s1} = 0.00013$ cm s^{-1}
$k_{s2} = 0.057$ cm s^{-1}	$(k^t_{s2})_{1H_2O} = 0.015$ cm s^{-1}	$k^t_{s2} = 0.0021$ cm s^{-1}
$\alpha_1^a = 0.47$	$(\alpha_1)_{1H_2O} = 0.45$	$\alpha_1 = 0.40$
$\alpha_2^a = 0.48$	$(\alpha_2)_{1H_2O} = 0.47$	$\alpha_2 = 0.48$
$A = 0.63\ \mu C^{-1}$ cm^2	$(A^t)_{1H_2O} = 0.55\ \mu C^{-1}$ cm^2	$A^t = 0.46\ \mu C^{-1}$ cm^2
$B = 0.34\ \mu C^{-1}$ cm^2	$(B^t)_{1H_2O} = 0.33\ \mu C^{-1}$ cm^2	$B^t = 0.30\ \mu C^{-1}$ cm^2

[a] $E_f^{\circ} = E^r_{1/2} + (RT/2F)\ln(D_O/D_R)^{1/2}$.

Comparison with theoretical models

The increase in the reduction rate of Zn^{2+} described in Figs. 1–4 appears to be related to interaction between the reactant and specifically adsorbed iodide rather than to the formation of halide complexes in the bulk of the solution ($E^r_{1/2}$ remains the same in the mixtures studied).

Several models have been devised to account for such an interaction [12–17]. They can be roughly classified into two groups:

Anion bridging models. These postulate the presence of an additional reaction pathway provided for by a previous chemical reaction between the reactant and the specifically adsorbed anions [25].

Electrostatic models. They describe the increase (or decrease) of reaction rate in terms of a purely electrical interaction between the activated complex and the specifically adsorbed anions [12,14–17].

Though the two kinds of models differ conceptually, in practice they can lead to similar formal kinetics, making distinction between them difficult; moreover, they do not exclude each other and they may be describing complementary elements of the same real situation.

Next we will consider the applicability of these models to our results.

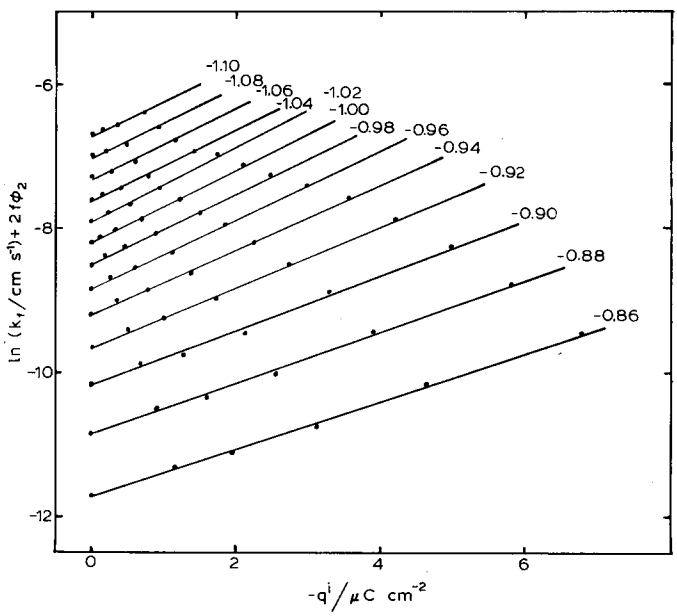

Fig. 4. As Fig. 2, after application of the diffuse double layer correction.

Anion bridged mechanism [13,25–27]

In the context of this model, the *overall* rate constant k_f is made up of a contribution from the reduction on a bare surface (k_b) and one from that of the halide catalyzed pathway (k_x).

Usually k_b is defined as the rate constant, at the potential considered, in the absence of specific adsorption (that is $k_b = k_0$ in our case), while k_x is characterized by its explicit dependence on the iodide surface activity ($a^s_{I^-}$): $k_x = k(E)(a^s_{I^-})^P/\gamma^{\neq}$, where P stands for the number of iodide ions entering the activated complex (or just the kinetic formal order in I^-) and $\gamma^{\neq}$ for the activity coefficient of the activated complex [27]. Although no unambiguous way exists in which k_0 and k_x should be added to give k_f, a natural (but crude) choice appears to be [9]:

$$k_f = (1-\theta)k_0 + \theta k_x \tag{4}$$

where θ is the fractional surface coverage, equal to q^i/q^i_{max}, with $q^i_{max} = -87\ \mu C\ cm^{-2}$. If $a^s_{I^-}$ is assumed to conform with a virial isotherm, and accordingly $\gamma^{\neq} = \exp(-2B_{\neq,I^-}q^i)$, then eqn. (4) can be rewritten:

$$k_f = (1-\theta)k_0 + \theta\left[k(E)(-q^i)^P \exp\left(2(PB_{I^-,I^-} - B_{\neq,I^-})(-q^i)\right)\right] \tag{5}$$

A test on the applicability of eq. (5) to our results can be readily obtained by plotting:

$$\ln\left[\frac{k_f-(1-\theta)k_0}{\theta}\right]_E - P\ln(-q^i) = A - P\ln(-q^i) \quad \text{vs.} \quad (-q^i)$$

for different values of P.

Figures 5 and 6 show such plots for $E = -0.9$ V and $E = -1.06$ V. No straight lines are obtained except for $P = 0$ and $E = -0.9$ V, and the unexpected sign should also be remarked of the slopes as $B_{I^-,I^-} > 0$ and $B_{\neq,I^-} < 0$ (at least for $P = 1$). The plots for $P = 0$ (meaningless within this formalism) are included as they would closely correspond to an alternative formulation [26] in which $(k_f - k_0)_E \propto (a^s_{I^-})^P$ is assumed. Similar results are obtained by plotting:

$$\ln\left[\frac{k^t_1-(1-\theta)k^t_0}{\theta}\right]_{E-\phi_2} - P\ln(-q^i) \quad \text{vs.} \quad (-q^i)$$

in order to account (at least partially) for the influence of adsorbed iodide on the non-catalytic pathway.

We conclude that our results cannot be satisfactorily explained by a parallel reaction mechanism.

Electrostatic models

In any consideration of the electrical interaction between adsorbed iodide and the activated complex, a central role is played by their mutual charges and due consideration of the multi-step nature of the Zn^{2+} reduction must be made.

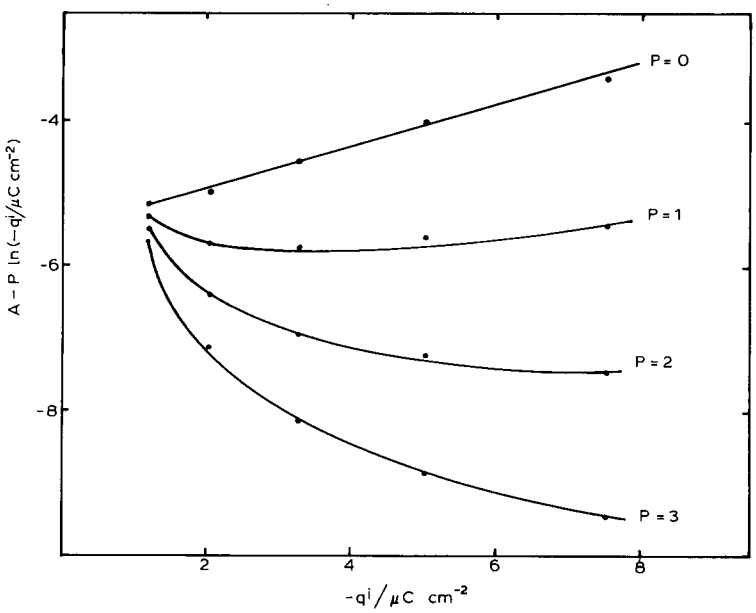

Fig. 5. Test of the applicability of eqn. (5) at $E = -0.90$ V vs. SSCE. For explanation see text.

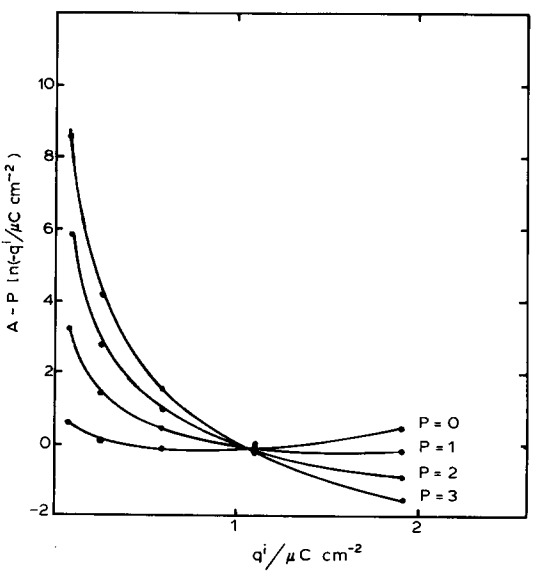

Fig. 6. As Fig. 5, at $E = -1.06$ V vs. SSCE.

Allowing for changes in the activity coefficients of reactants and activated complex, the rate constant for a mechanism of two one-electron-transfer steps can be expressed as follows [20]:

$$\frac{1}{k_f} = \frac{\exp(2f\phi^r)}{(\gamma_{Zn^{2+}})_b}\left(\frac{\gamma_1^{\neq} K_1^0}{k_1^0 \exp\left[-\alpha_1 f(\phi^M - \phi^r)\right]} + \frac{\gamma_2^{\neq} K_2^0}{k_2^0 \exp\left[-(1+\alpha_2) f(\phi^M - \phi^r)\right]}\right) \quad (6)$$

where K_i^0 represents the product of true equilibrium constants pertaining to any step preceding the ith electron transfer, ϕ^M and ϕ^r are the inner (averaged) potentials at the electrode and the reaction planes referred to the bulk of the solution, α_i, $\gamma_i^{\neq}$ and k_i^0, the true transfer coefficient, the activity of the activated complex and the potential independent rate constant for the ith electron transfer, respectively, and $(\gamma_{Zn^{2+}})_b$ the activity coefficient of Zn^{2+} in the bulk.

If the reaction plane is located at the Inner Helmholtz Plane (IHP):

$$\phi^r = \phi^{IHP} = \phi_2 + \lambda(\phi^M - \phi_2) + (1-\lambda) q^i / \overline{K}_2 \quad (7)$$

where $\overline{K}_2$ is the integral capacitance of the region situated between IHP and OHP, $\lambda = \overline{K}/\overline{K}_2$, $\overline{K}$ being the integral capacitance of the inner layer.

Comparison of Frumkin-corrected rate constants, at a given $E - \phi_2$, will prove to be a direct way to check some theoretical predictions. When the reaction plane is located at the IHP, from eqns. (6) and (7), with eqns. (1) and (2):

$$\ln(k_{10}^t/k_1^t)_{E-\phi_2} = A^t q^i = \ln(\gamma_1^{\neq}/\gamma_{10}^{\neq}) + (2-\alpha_1) f(1-\lambda) q^i/\overline{K}_2 \quad (8)$$

$$\ln(k_{20}^t/k_2^t)_{E-\phi_2} = B^t q^i = \ln(\gamma_2^{\neq}/\gamma_{20}^{\neq}) + (1-\alpha_2) f(1-\lambda) q^i/\overline{K}_2 \quad (9)$$

True transfer coefficients have been approximated by the Frumkin-corrected transfer coefficients.

Parsons model [12]

According to Parsons, while $\gamma^{\neq}$ can be considered independent of potential or of solution composition in the absence of specific adsorption, in its presence it may be described in terms of a virial coefficient as:

$$\gamma^{\neq} = \exp\left[-2B_{\neq,I^-}(-q^i)\right] \quad (10)$$

Furthermore, neglecting differences in inner potential between the reaction plane and the bulk:

$$\ln\left(\frac{k_i}{k_{i0}}\right)_E = 2B_{\neq,I^-}(-q^i) \quad (11)$$

where $B_{\neq,I^-}$ is estimated as: $B_{\neq,I^-}$,-di $= -z_{\neq} B_{I^-,I^-}$.

Comparison of eqns. (11) and (6) shows that within this model:

$$A = -2z_{\neq 1} B_{I^-,I^-} \quad \text{and} \quad B = -2z_{\neq 2} B_{I^-,I^-}$$

Values for B_{I^-,I^-} in the literature range from 2.20 to 5.00 nm^2 ion^{-1} [18] (Parsons used 3.50 nm^2 ion^{-1}), resulting in estimated charges of the activated complexes

between 2.3 and 1.0 for the first electron transfer, and between 1.2 and 0.5 for the second electron transfer, which compare satisfactorily with the expected values: $(2-\alpha_1)$ and $(1-\alpha_2)$.

Guidelli and Foresti model [14]

Guidelli and Foresti advocated the use of a rather simple electrostatic model in which the increase of the rate constant in the presence of iodide reflects only the corresponding changes in the average potential at the reaction plane. Equation (6) can be easily adapted to describe this model by making $\gamma_{i0}^{\neq} = \gamma_i^{\neq}$ and allowing for changes in ϕ^r.

The quotient between Frumkin-corrected rate constants reads:

$$\ln(k_{10}^{\iota}/k_1^{\iota})_{E-\phi_2} = (2-\alpha_1) f 4\pi l q^{i}/\epsilon \tag{12}$$

$$\ln(k_{20}^{\iota}/k_2^{\iota})_{E-\phi_2} + (1-\alpha_2) f 4\pi l q^{i}/\epsilon \tag{13}$$

where: $l = \beta(1 - x_{\neq}/\delta)$ for $x_{\neq} \geqslant \beta$ and $l = (\gamma/\delta)x_{\neq}$ for $x_{\neq} \leqslant \beta$; β, δ and $x_{\neq}$ are the distances of the IHP, OHP and the reaction plane from the electrode, $\gamma = \delta - \beta$.

Introducing [14]: $\beta/\delta = 0.6$, $\gamma = 0.16$ nm, $\epsilon = 4.5$ and recalling the values of A^{ι}, B^{ι}, α_1 and α_2 (Table 1), two sets of reaction plane locations can be derived: derived:

$x_{\neq} \geqslant \beta \qquad x_{\neq,1} = 0.35$ nm $\qquad x_{\neq,2} = 0.28$ nm

$x_{\neq} \leqslant \beta \qquad x_{\neq,1} = 0.07$ nm $\qquad x_{\neq,2} = 0.18$ nm

Though both sets give reasonable values for the reaction plane location, the first one $(x_{\neq} \geqslant \beta)$ may appear more realistic on the basis of a progressive penetration of the reacting particle into the inner layer along the reaction coordinate.

Levine and Fawcett model [15,28]

In the Levine and Fawcett model, the quotient between the activity coefficients of the activated complex in the presence and absence of specific adsorption is associated with the difference in exclusion disc potential at the reaction plane (which is identified with the IHP) and is estimated according to [15]:

$$\ln(\gamma^{\neq}/\gamma_0^{\neq}) = -z_{\neq} g_{\neq} f(1-\lambda) q^{i}/\bar{K}_2 \tag{14}$$

where $g_{\neq} \sim 1$.

Introducing (14) in eqs. (8) and (9) we obtain:

$$(2 - \alpha_1 - z_{\neq 1}) = 0.46\, \bar{K}_2/f(1-\lambda) \tag{15}$$

$$(1 - \alpha_2 - z_{\neq 2}) = 0.30\, \bar{K}_2/f(1-\lambda) \tag{16}$$

neglecting an entropic term [15], due to the low coverages encountered in this work.

After numerical substitution of $\bar{K}_2/f(1-\lambda) \sim 2.2\ \mu C\ cm^{-2}$ [18], the following charges of the activated complexes are found: $z_{\neq 1} = 0.6$ and $z_{\neq 2} = -0.1$, respectively. Similar anomalously low values were found previously [15] in the analysis of the H^+ reduction and were ascribed to a decrease of the "effective charge" of the

reactant due to its interactions with neighbouring anions. Even if a similar line of reasoning could be introduced in our case, it seems that the model itself is bound to lead to values of $z_{\neq} \ll (z - \alpha)$ when dealing with a significant catalysis of a cation reduction.

Explicit consideration of ion-pairing between the reactant and specifically adsorbed iodide leads to somewhat different equations describing the iodide catalysis [28]:

$$\ln(k_{10}^{t}/k_{1}^{t})_{E-\phi_2} = (2-\alpha_1)f(1-\lambda)q^{i}/\bar{K}_2 + (2-\alpha_1)f\phi_{disc} + (1-\alpha_1)\xi_{2,-1}/RT + \alpha_1\xi_{1,-1}/RT \quad (17)$$

$$\ln(k_{20}^{t}/k_{2}^{t})_{E-\phi_2} = (1-\alpha_2)f(1-\lambda)q^{i}/\bar{K}_2 + (1-\alpha_2)f\phi_{disc} + (1-\alpha_2)\xi_{1,-1}/RT \quad (18)$$

The term ξ_{z_i,z_j} accounts for the ion-pairing contribution to the discreteness-of-charge energy:

$$\xi_{z_i,z_j} = z_i z_j F e_0 \int_a^{r_{ij}} G_{ij}(r)\phi_0(r)\mathrm{d}r \quad (19)$$

where r is the distance from the reacting ion i along the IHP, e_0 the electron charge, $G_{ij}\mathrm{d}r$ the probability of finding a j ion in a circular ring of thickness $\mathrm{d}r$ at a distance r from i; $z_i e_0 \phi_0(r)$ is the change in potential at r due to a point charge $z_i e_0$ keeping a fixed charge distribution on the IHP, a the exclusion disc radius and r_{ij} the distance at which G_{ij} displays a minimum. Figure 7 shows calculated $\xi_{i,j}/RT$ values as a

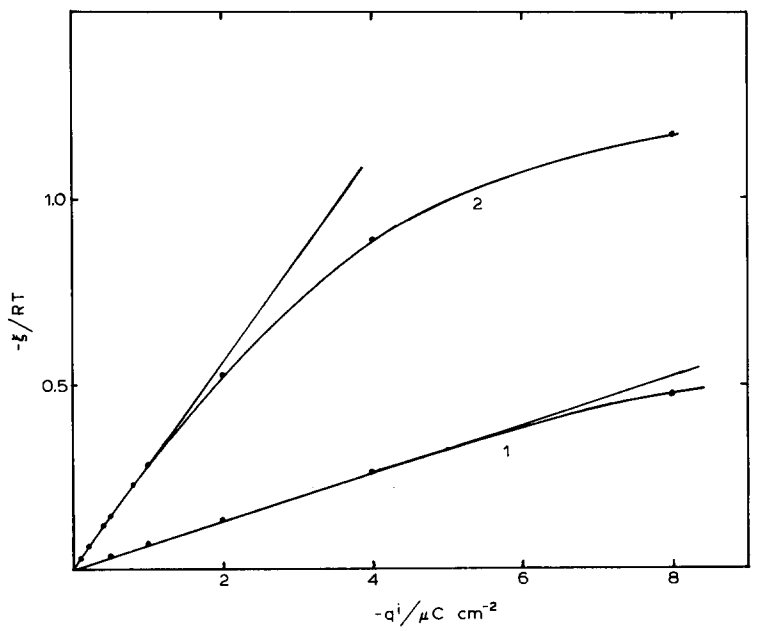

Fig. 7. Test of the applicability of the Levine and Fawcett model. For explanation see text.

function of q^i, assuming $a = 0.5$ nm (both curves), $r_{1,-1} = 0.8$ nm (curve 1), and $r_{2,-1} = 0.95$ nm (curve 2), other parameters being the same as in [28]. At low q^i values:

$$\xi_{2,-1}/RT = 0.28\, q^i \qquad \text{and} \qquad \xi_{1,-1}/RT = 0.07\, q^i.$$

The disc potential was evaluated according to [28]:

$$\phi_{\text{disc}} = \frac{-2\pi\delta q^i}{(\epsilon_{\text{mr}} + \epsilon_{\text{rd}})}\left[1 - \frac{8A}{\pi^2}\sum_{\mu=1}^{\infty}\frac{1}{2\mu-1}K_1[(2\mu-1)Q]\right]$$

with $\delta = 0.55$ nm, $\epsilon_{\text{mr}} = 10.4$ and $\epsilon_{\text{rd}} = 18.3$ (dielectric constants of the inner and outer regions of the inner layer), $Q = \pi r_{i,j}/\delta$ and K_1 being the Bessel function of second kind with imaginary argument and first order. After numerical substitution in eqns. (17) and (18), the values

$$\ln(k^t_{10}/k^t_1) = 0.24\, q^i \qquad \text{and} \qquad \ln(k^t_{20}/k^t_2) = 0.06\, q^i$$

are obtained, which should be compared with $A^t = 0.55$ and $B^t = 0.33$, respectively (Table 1). So, inclusion of ion pairing significantly improves the agreement between model and experiment. Lowering the selected a value would increase the predicted A^t and B^t values (when $q^i \to 0$), but at the cost of a more pronounced departure of the $\ln(k^t_{10}/k^t_i)_{E-\phi_2}$ vs. q^i plots from linearity.

Guidelli model [16,29]

Guidelli's model differs essentially from that of Fawcett and Levine by the neglect of the perturbation in the charge density due to adsorbed anions by the activated complex, by equating its charge directly to $(z - \alpha)$ and by assuming a value close to 1 for the local dielectric constant.

Comparison with experiment can be readily obtained by [16]:

$$\frac{\partial}{\partial q^i}\left[\ln\frac{k^t_1}{k^t_{10}}\right]_{E-\phi_2} = 4\pi f(\alpha'_1 - 2)\frac{\beta\gamma}{\delta}\frac{1 - {}^1g}{\epsilon} \tag{20}$$

$$\frac{\partial}{\partial q^i}\left[\ln\frac{k^t_2}{k^t_{20}}\right]_{E-\phi_2} = 4\pi f(\alpha'_2 - 1)\frac{\beta\gamma}{\delta}\frac{1 - {}^1g}{\epsilon} \tag{21}$$

where $\alpha'_i = [\alpha_i - z_i(1 - x_{\neq,i}/\delta)]/(x_{\neq,i}/\delta)$. The function $(1 - {}^1g)$ is introduced to take account of the difference between average and local potential at $x_{\neq}$.

Substitution of $x_{\neq,i}/\delta = \beta/\delta = 0.6$, $(\alpha'_1 - 2) = -2.7$, $(\alpha'_2 - 1) = -0.9$ and $\gamma = 0.16$ nm leads to:

$$\frac{\partial}{\partial q^i}\left[\ln\frac{k^t_1}{k^t_{10}}\right]_{E-\phi_2} = -0.29(1 - {}^1g) \quad \mu\text{C}^{-1}\,\text{cm}^2$$

$$\frac{\partial}{\partial q^i}\left[\ln\frac{k^t_2}{k^t_{20}}\right]_{E-\phi_2} = -0.098(1 - {}^1g) \quad \mu\text{C}^{-1}\,\text{cm}^2$$

If we make the reasonable choice $(1 - {}^1g) \times 0.1$ [16,30], the predicted slopes are still at least one order of magnitude smaller than the experimental ones. A similar disparity occurred in connection with the H^+ reduction, which was explained [16] as being due to a particularly low value of the exclusion disc radius around an unsolvated proton. Such a possibility is not likely to apply in our case ($r_{I^-} \sim 0.22$ nm, $r_{Zn^{2+}} \sim 0.074$ nm, $a \sim 0.3$ nm), unless ${}^1g$ should take an extremely low value (or a meaningless negative one) which seems far from the theoretical prediction.

It is also interesting to note that the parameter α_i', which is referred to in [16] as a true transfer coefficient, takes a negative value for the first electron transfer and a very low one for the second.

As in the preceding model, consideration of ionic pairing between reactant and adsorbed iodide gives a more reasonable correlation between experiment and theory. According to Guidelli [29]:

$$\frac{\partial}{\partial q^i}\left[\ln \frac{k_1^t}{k_{10}^t}\right]_{E-\phi_2} = (\alpha_1' - 2) h_{2,-1} f \tag{22}$$

$$\frac{\partial}{\partial q^i}\left[\ln \frac{k_2^t}{k_{20}^t}\right]_{E-\phi_2} = (\alpha_2' - 1) h_{1,-1} f \tag{23}$$

where:

$$h_{z_i,z_j} = \frac{2\pi}{\epsilon}\left(\frac{8}{a\delta}\right)^{1/2} \sin^2\left(\frac{\pi\beta}{\delta}\right) \exp\left(-\frac{\pi a}{\delta}\right) \int_a^{r_{ij}} r \exp\left(\frac{-z_i e_0 \phi_j(r)}{kT}\right) dr \tag{24}$$

The electrical potential produced by an adsorbed ion j and by its infinite images is approximated by:

$$\phi_j(r) = \frac{z_j e_0}{\epsilon}\left(\frac{\gamma}{r\delta}\right)^{1/2} \sin^2\left(\frac{\pi\beta}{\delta}\right) \exp\left(-\frac{\pi r}{\delta}\right)$$

The integrand in eqn. (24) reaches a minimum at $r_{2,-1} = 0.98$ nm and $r_{1,-1} = 0.88$ nm. If $\beta = 0.3$ nm, $\delta = 0.4$ nm and $\epsilon = 1$ are selected [29], theoretical predictions fit our results when $a = 0.66$ nm for the first electron transfer and $a = 0.57$ nm for the second.

Krylov et al. model [17]

More recently Krylov et al. [17] have developed an electrostatic model which, allowing for a varying location of the reaction plane, gives a quantitative explanation for the influence of iodide ions on the kinetics of H^+ reduction. Neglecting double-layer diffuseness and approximating $1 - \theta \sim 1$, the quotient between rate constants is expressed as:

$$\ln\left(\frac{k_{i0}}{k_i}\right)_E = \Omega_{z_i - \alpha_i}/kT \tag{25}$$

For a hexagonal lattice distribution of the adsorbed iodide:

$$\Omega_{z_i-\alpha_i} = -\frac{12\, e_0^2(z_i-\alpha_i)}{\epsilon\delta}\left(\sum_{m=0}^{\infty}\sum_{p=1}^{\infty}\sin(\pi p\beta/\delta)\sin\left(\frac{\pi p(x_0+\beta)}{\delta}\right)\right.$$

$$\times K_0\left(\frac{\pi p r^*\sqrt{3}}{\delta}\right)\left(m+\tfrac{1}{3}\right)\Bigg) + \sum_{m=1}^{\infty}\sum_{n=1}^{3m}\sum_{p=1}^{\infty}\sin\left(\frac{\pi p\beta}{\delta}\right)\sin\left(\frac{\pi p(x_0+\beta)}{\delta}\right)$$

$$\times K_0\left(\frac{\pi p r^*}{\delta}\left((3m+1)\left(m+\tfrac{1}{3}-n\right)-n^2\right)\right) \qquad (26)$$

where x_0 is the distance of the reacting plane from the IHP, and r^* the closest distance between two adsorbed ions: $r^* = (\frac{1}{2}\sqrt{3}\,\Gamma_{I^-}^{i})^{-1/2}$.

Figure 8 shows the calculated $\Omega_{z_i-\alpha_i}/kT$ values for $\beta = 0.25$ nm, $\delta = 0.5$ nm, $x_0 = 0.05$ nm and $K_0(x)$ estimated by $\sqrt{\pi/2x}\ e^{-x}$ as a function of $-q^i$.

A non-linear dependence is observed, at least for the q^i range covered in this work. The predicted accelerating effect is lower than the experimental one, but the slopes of the plots display the correct order of magnitude for $x_0 \leqslant 0.1$ nm and $|q^i| > 6\ \mu C\ cm^{-2}$.

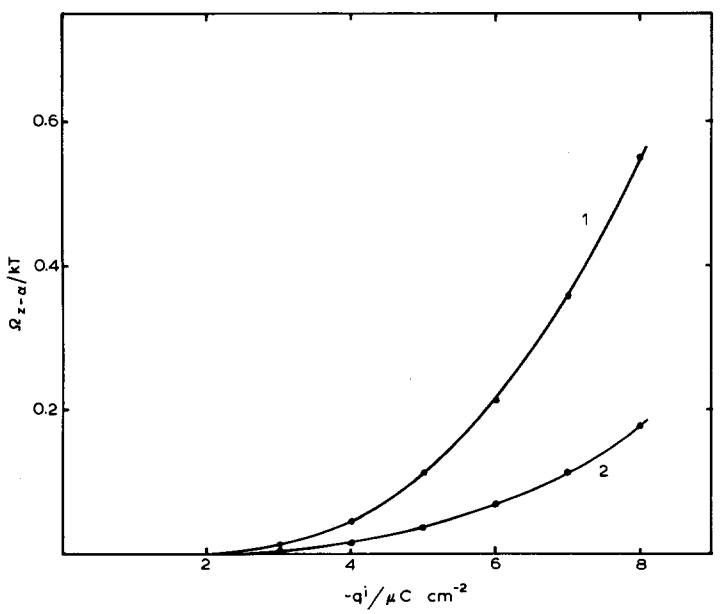

Fig. 8. Test of the applicability of the Krylov et al. model. Curve 1: 1st, curve 2: 2nd electron transfer. For explanation see text.

TABLE 2

Degree of applicability of the electrostatic models to our data

	P[12]	GF[14]	FL[15]	FL[28]	G[16]	G[29]	KKF[17]
Higher acceleration of the 1st step	+	+	+	+	+	+	+
Linear relationship between ln k_i and q^i	+	+	+	only low q^i	+	+	−
Correct order of magnitude of A^t, B^t	+	+	−	only low q^i	−	+	only high q^i

CONCLUSIONS

A preliminary consideration of the iodide catalysis of the Zn^{2+} reduction at the most negative potentials (where the first electron transfer is rate determining) allowed us to split up the increase in the overall rate constant into separate contributions from the two electron-transfer steps. We could then conclude that both steps obey a common rate law, i.e. $\ln k_i$ being proportional to the amount of specifically adsorbed iodide, with the first electron transfer undergoing a higher acceleration than the second one.

While the anion bridged mechanism failed to account for such behaviour, the models of Parsons [12], Guidelli and Foresti [14] and Guidelli [29] were able to fit our results quantitatively. It may be interesting to note that, in spite of the remarkably detailed nature of some models considered here (e.g. those of Krylov et al. [17] or Fawcett and Levine [15,28]), a similar (and often better) correlation between theory and experiment could be reached by much less sophisticated approaches like that of Guidelli and Foresti [14].

On the basis of an electrostatic interaction between reactants and adsorbed iodide the quotient A^t/B^t could be expected to remain close to 3 (i.e. $(2 - \alpha_1)/(1 - \alpha_2)$), but in fact a value of ~ 1.5 was found. Two explanations have been offered to account for such a result:

(i) Different reaction planes for each electron transfer step, the reaction plane for the second electron transfer being closer to the IHP than the reaction plane for the first one.

(ii) A smaller exclusion disc radius for Zn^+ than for Zn^{2+}.

Both statements can be regarded as complementary and ultimately related to the lower hydration of Zn^+ as compared to Zn^{2+} [20].

Table 2 summarizes the degree of applicability of the electrostatic models to our data.

ACKNOWLEDGEMENT

The technical assistance of Mr. J.M. Oostveen is gratefully acknowledged.

REFERENCES

1 V.V. Losev in B.E. Conway and J.O'M. Bockris (Eds.), Modern Aspects of Electrochemistry, Vol. 7, Butterworths, London, 1972, pp. 314–398.
2 G. Salié, Z. Phys. Chem., 244 (1970) 1.
3 T. Hurlen and E. Eriksrud, J. Electroanal. Chem., 45 (1973) 405.
4 F. van der Pol, M. Sluyters-Rehbach and J.H. Sluyters, J. Electroanal. Chem., 58 (1975) 177.
5 J.E.B. Randles and K.W. Somerton, Trans. Faraday Soc., 48 (1952) 951.
6 J. Blackledge and N.S. Hush, J. Electroanal. Chem., 5 (1963) 435.
7 A. Hamelin, Electrochim. Acta, 9 (1964) 289.
8 T. Kambara and T. Ishi, Rev. Polarography, 9 (1961) 30.
9 R. Tamamushi, K. Ishibashi and N. Tanaka, Z. Phys. Chem. N.F., 35 (1962) 209.
10 P. Teppema, M. Sluyters-Rehbach and J.H. Sluyters, J. Electroanal. Chem., 16 (1968) 165.
11 M. Sluyters-Rehbach, J.S.M.C. Breukel and J.H. Sluyters, J. Electroanal. Chem., 19 (1968) 85.
12 R. Parsons, J. Electroanal. Chem., 21 (1969) 35.
13 L. Pospíšil and R. de Levie, J. Electroanal. Chem., 25 (1970) 245.
14 R. Guidelli and M.L. Foresti, Electrochim. Acta, 18 (1973) 301.
15 W.R. Fawcett and S. Levine, J. Electroanal. Chem., 43 (1973) 175.
16 R. Guidelli, J. Electroanal. Chem., 53 (1974) 205.
17 V.S. Krylov, V.A. Kiryanov and I.F. Fishtik, J. Electroanal. Chem., 109 (1980) 115.
18 E. Eriksrud, J. Electroanal. Chem., 76 (1977) 27.
19 C.P.M. Bongenaar, M. Sluyters-Rehbach and J.H. Sluyters, J. Electroanal. Chem., 109 (1980) 23.
20 R. Andreu, M. Sluyters-Rehbach, A.G. Remijnse and J.H. Sluyters, J. Electroanal. Chem., 134 (1982) 101.
21 A.G. Stromberg, Dokl. Akad. Nauk, U.S.S.R., 85 (1952) 831.
22 D.C. Grahame, J. Am. Chem. Soc., 80 (1958) 4201.
23 E. Dutkiewicz and R. Parsons, J. Electroanal. Chem., 11 (1966) 100.
24 D.M. Mohilner, in A.J. Bard (Ed.), Electroanalytical Chemistry, Vol. 1, Marcel Dekker, New York, 1966, pp. 241–409.
25 R. de Levie, J. Electrochem. Soc., 118 (1971) C185.
26 R. de Levie and L. Pospíšil, J. Electroanal. Chem., 25 (1970) 340.
27 F.C. Anson, J. Electroanal. Chem., 47 (1973) 279.
28 W.R. Fawcett and S. Levine, J. Electroanal. Chem., 65 (1975) 505.
29 R. Guidelli, J. Electroanal. Chem., 74 (1976) 347.
30 S. Levine, J. Mingins and G.M. Bell, Can. J. Chem., 43 (1965) 2834.